Hour-long continuous operation of a tabletop soft x-ray laser at 50-100 Hz repetition rate

Brendan A. Reagan,[1,2,*] Wei Li,[1,2] Lukasz Urbanski,[1,2] Keith A. Wernsing,[1,2] Chase Salsbury,[1,2,3] Cory Baumgarten,[1,4] Mario C. Marconi,[1,2] Carmen. S. Menoni,[1,2] and Jorge J. Rocca[1,2,4]

[1]*NSF Engineering Research Center for Extreme Ultraviolet Science and Technology, Fort Collins, CO 80523, USA*
[2]*Department of Electrical and Computer Engineering, Colorado State University, Fort Collins, CO 80523, USA*
[3]*Permanent address: College of Optical Sciences, University of Arizona, Tucson, AZ 85721, USA*
[4]*Department of Physics, Colorado State University, Fort Collins, CO 80523, USA*
[*]*breagan@engr.colostate.edu*

Abstract: We report the uninterrupted operation of an 18.9 nm wavelength tabletop soft x-ray laser at 100 Hz repetition rate for extended periods of time. An average power of about 0.1 mW was obtained by irradiating a Mo target with pulses from a compact diode-pumped chirped pulse amplification Yb:YAG laser. Series of up to 1.8 x 10^5 consecutive laser pulses of ~1 μJ energy were generated by displacing the surface of a high shot-capacity rotating molybdenum target by ~2 μm between laser shots. As a proof-of-principle demonstration of the use of this compact ultrashort wavelength laser in applications requiring a high average power coherent beam, we lithographically printed an array of nanometer-scale features using coherent Talbot self-imaging.

OCIS codes: (140.7240) UV, EUV, and X-ray lasers; (340.7480) X-rays, soft x-rays, extreme ultraviolet (EUV); (140.3480) Lasers, diode-pumped.

References and links

1. J. Filevich, K. Kanizay, M. C. Marconi, J. L. A. Chilla, and J. J. Rocca, "Dense plasma diagnostics with an amplitude-division soft-x-ray laser interferometer based on diffraction gratings," Opt. Lett. **25**(5), 356–358 (2000).
2. T. Suemoto, K. Terakawa, Y. Ochi, T. Tomita, M. Yamamoto, N. Hasegawa, M. Deki, Y. Minami, and T. Kawachi, "Single-shot picosecond interferometry with one-nanometer resolution for dynamical surface morphology using a soft X-ray laser," Opt. Express **18**(13), 14114–14122 (2010).
3. G. Vaschenko, C. Brewer, F. Brizuela, Y. Wang, M. A. Larotonda, B. M. Luther, M. C. Marconi, J. J. Rocca, C. S. Menoni, E. H. Anderson, W. Chao, B. D. Harteneck, J. A. Liddle, Y. Liu, and D. T. Attwood, "Sub-38 nm resolution tabletop microscopy with 13 nm wavelength laser light," Opt. Lett. **31**(9), 1214–1216 (2006).
4. S. Carbajo, I. D. Howlett, F. Brizuela, K. S. Buchanan, M. C. Marconi, W. Chao, E. H. Anderson, I. Artioukov, A. Vinogradov, J. J. Rocca, and C. S. Menoni, "Sequential single-shot imaging of nanoscale dynamic interactions with a table-top soft x-ray laser," Opt. Lett. **37**(14), 2994–2996 (2012).
5. F. Brizuela, Y. Wang, C. A. Brewer, F. Pedaci, W. Chao, E. H. Anderson, Y. Liu, K. A. Goldberg, P. Naulleau, P. Wachulak, M. C. Marconi, D. T. Attwood, J. J. Rocca, and C. S. Menoni, "Microscopy of extreme ultraviolet lithography masks with 13.2 nm tabletop laser illumination," Opt. Lett. **34**(3), 271–273 (2009).
6. I. Kuznetsov, J. Filevich, F. Dong, W. L. Chao, E. H. Anderson, E. R. Bernstein, D. C. Crick, J. J. Rocca, and C. S. Menoni, "Nanoscale 3D composition imaging by soft x-ray laser ablation mass spectrometry," 2012 Conference on Lasers and Electro-Optics (CLEO) (2012).
7. B. Zielbauer, J. Habib, S. Kazamias, O. Guilbaud, M. Pittman, D. Ros, M.-A. H. du Penhoat, A. Touati, C. Le Sech, and E. Porcel, "Strand breaks in DNA samples induced with LASERIX," in *X-Ray Lasers 2008* (Springer, 2009), pp. 409–411.
8. H. Bravo, B. T. Szapiro, P. W. Wachulak, M. C. Marconi, W. Chao, E. H. Anderson, C. S. Menoni, and J. J. Rocca, "Demonstration of nanomachining with focused extreme ultraviolet laser beams," IEEE J. Sel. Top. Quantum Electron. **18**(1), 443–448 (2012).
9. L. Urbanski, A. Isoyan, A. Stein, J. J. Rocca, C. S. Menoni, and M. C. Marconi, "Defect-tolerant extreme ultraviolet nanoscale printing," Opt. Lett. **37**(17), 3633–3635 (2012).
10. B. R. Benware, C. D. Macchietto, C. H. Moreno, and J. J. Rocca, "Demonstration of a high average power tabletop soft X-ray laser," Phys. Rev. Lett. **81**(26), 5804–5807 (1998).
11. C. D. Macchietto, B. R. Benware, and J. J. Rocca, "Generation of millijoule-level soft-x-ray laser pulses at a 4-Hz repetition rate in a highly saturated tabletop capillary discharge amplifier," Opt. Lett. **24**(16), 1115–1117 (1999).

#198284 - $15.00 USD Received 25 Sep 2013; revised 4 Nov 2013; accepted 4 Nov 2013; published 11 Nov 2013

12. Y. Wang, M. A. Larotonda, B. M. Luther, D. Alessi, M. Berrill, V. N. Shlyaptsev, and J. J. Rocca, "Demonstration of high-repetition-rate tabletop soft-x-ray lasers with saturated output at wavelengths down to 13.9 nm and gain down to 10.9 nm," Phys. Rev. A **72**(5), 053807 (2005).
13. D. H. Martz, D. Alessi, B. M. Luther, Y. Wang, D. Kemp, M. Berrill, and J. J. Rocca, "High-energy 13.9 nm table-top soft-x-ray laser at 2.5 Hz repetition rate excited by a slab-pumped Ti: sapphire laser," Opt. Lett. **35**(10), 1632–1634 (2010).
14. M. Grünig, C. Imesch, F. Staub, and J. E. Balmer, "Saturated X-ray lasing in Ni-like Sn at 11.9 nm using the GRIP scheme," Opt. Commun. **282**(2), 267–271 (2009).
15. H. T. Kim, I. W. Choi, N. Hafz, J. H. Sung, T. J. Yu, K.-H. Hong, T. M. Jeong, Y.-C. Noh, D.-K. Ko, K. A. Janulewicz, J. Tümmler, P. Nickles, W. Sandner, and J. Lee, "Demonstration of a saturated Ni-like Ag x-ray laser pumped by a single profiled laser pulse from a 10-Hz Ti: sapphire laser system," Phys. Rev. A **77**(2), 023807 (2008).
16. D. Zimmer, B. Zielbauer, M. Pittman, O. Guilbaud, J. Habib, S. Kazamias, D. Ros, V. Bagnoud, and T. Kuehl, "Optimization of a tabletop high-repetition-rate soft x-ray laser pumped in double-pulse single-beam grazing incidence," Opt. Lett. **35**(4), 450–452 (2010).
17. D. Alessi, Y. Wang, B. M. Luther, L. Yin, D. H. Martz, M. R. Woolston, Y. Liu, M. Berrill, and J. J. Rocca, "Efficient excitation of gain-saturated sub-9-nm-wavelength tabletop soft-X-ray lasers and lasing down to 7.36 nm," Phys. Rev. X **1**, 021023 (2011).
18. B. A. Reagan, K. A. Wernsing, A. H. Curtis, F. J. Furch, B. M. Luther, D. Patel, C. S. Menoni, and J. J. Rocca, "Demonstration of a 100 Hz repetition rate gain-saturated diode-pumped table-top soft x-ray laser," Opt. Lett. **37**(17), 3624–3626 (2012).
19. M. Nishikino, Y. Ochi, N. Hasegawa, T. Kawachi, H. Yamatani, T. Ohba, T. Kaihori, and K. Nagashima, "Demonstration of a highly coherent 13.9 nm x-ray laser from a silver tape target," Rev. Sci. Instrum. **80**(11), 116102 (2009).
20. A. Weith, M. A. Larotonda, Y. Wang, B. M. Luther, D. Alessi, M. C. Marconi, J. J. Rocca, and J. Dunn, "Continuous high-repetition-rate operation of collisional soft-x-ray lasers with solid targets," Opt. Lett. **31**(13), 1994–1996 (2006).
21. B. Zielbauer, D. Zimmer, J. Habib, O. Guilbaud, S. Kazamias, M. Pittman, and D. Ros, "Stable and fully controlled long-time operation of a soft X-ray laser for user application experiments," Appl. Phys. B **100**(4), 731–736 (2010).
22. A. H. Curtis, B. A. Reagan, K. A. Wernsing, F. J. Furch, B. M. Luther, and J. J. Rocca, "Demonstration of a compact 100 Hz, 0.1 J, diode-pumped picosecond laser," Opt. Lett. **36**(11), 2164–2166 (2011).
23. B. A. Reagan, A. H. Curtis, K. A. Wernsing, F. J. Furch, B. M. Luther, and J. J. Rocca, "Development of high energy diode-pumped thick-disk Yb: YAG chirped-pulse-amplification lasers," IEEE J. Quantum Electron. **48**(6), 827–835 (2012).
24. R. Keenan, J. Dunn, P. K. Patel, D. F. Price, R. F. Smith, and V. N. Shlyaptsev, "High-repetition-rate grazing-incidence pumped x-ray laser operating at 18.9 nm," Phys. Rev. Lett. **94**(10), 103901 (2005).
25. B. M. Luther, Y. Wang, M. A. Larotonda, D. Alessi, M. Berrill, M. C. Marconi, J. J. Rocca, and V. N. Shlyaptsev, "Saturated high-repetition-rate 18.9-nm tabletop laser in nickellike molybdenum," Opt. Lett. **30**(2), 165–167 (2005).
26. Y. Wang, E. Granados, F. Pedaci, D. Alessi, B. Luther, M. Berrill, and J. J. Rocca, "Phase-coherent, injection-seeded, table-top soft-X-ray lasers at 18.9 nm and 13.9 nm," Nat. Photonics **2**(2), 94–98 (2008).
27. M. Nishikino, M. Tanaka, K. Nagashima, M. Kishimoto, M. Kado, T. Kawachi, K. Sukegawa, Y. Ochi, N. Hasegawa, and Y. Kato, "Demonstration of a soft-x-ray laser at 13.9 nm with full spatial coherence," Phys. Rev. A **68**(6), 061802 (2003).
28. A. Isoyan, F. Jiang, Y. Cheng, F. Cerrina, P. Wachulak, L. Urbanski, J. Rocca, C. Menoni, and M. Marconi, "Talbot lithography: Self-imaging of complex structures," J. Vac. Sci. Technol. B **27**(6), 2931–2937 (2009).
29. C. Zanke, M. H. Qi, and H. I. Smith, "Large-area patterning for photonic crystals via coherent diffraction lithography," J. Vac. Sci. Technol. B **22**(6), 3352–3355 (2004).

1. Introduction

Applications of coherent soft x-ray radiation made possible by compact soft x-ray lasers (SXRLs) have been demonstrated in several areas and have a promising future in basic research and technology. These applications include soft x-ray interferometry to study dense plasmas [1] and surface dynamics [2], ultra-high resolution microscopy [3, 4], actinic defect inspection of the next generation of lithographic masks [5], nanometer-scale probing of surfaces [6], studies of radiation damage in DNA [7], the fabrication of very fine features through laser nano-machining [8], and defect-free coherent lithography [9]. Several of these applications, such as nano-machining and interferometric lithography, that require a high photon flux were enabled by capillary discharge Ne-like Ar SXRLs operating at $\lambda = 46.9$nm which are capable of producing milliwatt average powers continuously for long operating durations [10, 11]. Although several compact, gain-saturated, sub-20nm wavelength SXRLs based on laser produced plasmas from solid targets have been demonstrated at wavelengths as short as 8.8 nm [12–17], including the recent realization of lasers producing greater than 0.1

#198284 - $15.00 USD Received 25 Sep 2013; revised 4 Nov 2013; accepted 4 Nov 2013; published 11 Nov 2013

mW average powers at λ = 18.9nm [18], long term high average power operation has not been demonstrated. Several target geometries have been developed or proposed with the goal of extending the time period of continuous soft x-ray laser operation, including tape targets [19], rotating targets [20], and slowly moving slab targets [21]. For example, the use of rotating helical targets has enabled nano-scale imaging experiments requiring exposures of the order of 20 seconds at 5 Hz repetition rate [5]. However long term operation at more demanding (>50 Hz) repetition rates had not yet been demonstrated. In this paper, we report the continuous, long-term, high average power operation of a compact λ = 18.9nm laser at repetition rates up to 100 Hz. Combining a diode-pumped chirped pulse amplification (CPA) driver laser with a high shot capacity rotating molybdenum target we produced λ = 18.9 nm laser pulses of ~1 μJ energy at 100 Hz repetition rate for 30 minutes without interruption, and at 50 Hz repetition rate for over 1 hour. As a demonstration of the enabling power of this laser for applications requiring a high photon flux, we made use of it as a coherent illumination source to print an array of nanometer-scale features by coherent lithography exploiting the Talbot self-imaging effect.

2. Compact high repetition rate soft x-ray laser setup

Figure 1(a) shows the layout of the tabletop SXRL. The SXRL is driven by a λ = 1.03 μm CPA laser system based on cryogenic Yb:YAG amplifiers that is entirely pumped by laser diodes. This driver laser system, discussed in [18, 22, 23], produces 1 Joule, 5 ps FWHM duration pulses at 100 Hz repetition rate. Laser pulses are focused in vacuum using the combination of a cylindrical lens and cylindrical mirror forming an ~6 mm long line focus of 30 μm FWHM width. The beam is focused on to the target at a grazing incidence angle of 29° in order to preferentially heat the plasma density region optimal for soft x-ray amplification [24, 25]. The plasma is created and heated by single temporally-tailored laser pulses of 0.9 J energy with 6 ps FWHM main peak preceded by an intentionally added nanoseconds duration pedestal with ~10^{-3} relative intensity as described in [18].

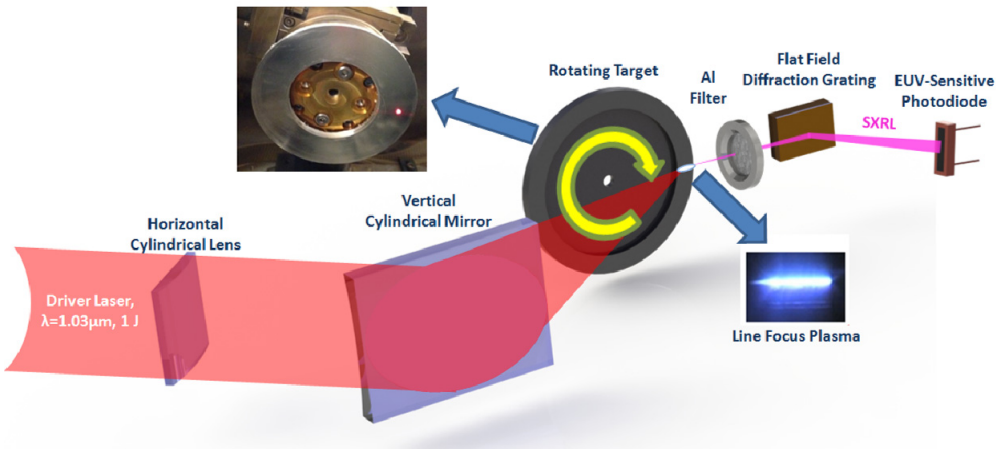

Fig. 1. Setup for generating the continuously operating SXRL. Driver laser pulses exiting the pulse compressor are focused into a line on the target at grazing incidence using cylindrical optics. Photographs of the high shot capacity target and the line focus plasma amplifier are shown inset.

The high shot capacity rotating target is shown in the photograph inset in Fig. 1. The target consists of a disk of molybdenum, the face of which is flat and mechanically polished. The target is mounted to a vacuum compatible rotation stage driven by a computer-controlled stepper motor. The rotation stage itself is mounted on XY translation stages to allow precise positioning of the target in the line focus of the driving laser. The laser line focus partially clips the edge of the target in an effort to minimize absorption of the generated SXRL in the colder plasma that would otherwise be present at the end of the line focus. The target used in

#198284 - $15.00 USD Received 25 Sep 2013; revised 4 Nov 2013; accepted 4 Nov 2013; published 11 Nov 2013

the experiments has a circumference of 314 mm (100 mm diameter), which when rotated such that the distance between successive shots is 2 μm, allows more than 150,000 shots per rotation. Mo is particularly well suited for withstanding many shots on a single spot without sustaining large surface deformation due to its very high melting point [16], which allows the use of the target for multiple rotations. Low melting point target materials, such as Cd or Sn would require greater translation between shots.

3. Continuous high repetition rate soft x-ray laser performance

The soft x-ray laser output was optimized by measuring the on-axis EUV spectral emission with a flat-field grazing incidence variable spaced diffraction grating and an x-ray sensitive CCD. Multiple thin aluminum foils were used to reject visible plasma emission and stray light from the driver laser, as well as to attenuate the SXRL to prevent detector saturation. The transmissivity of these filters at $\lambda = 18.9$ nm was calibrated in situ using the soft x-ray laser to allow for pulse energy measurements. Figures 2(a) and 2(b) show a single shot spectrum of a Mo plasma with strong lasing on the $4d^1S_0 \rightarrow 4p^1P_1$ transition of Ni-like Mo ions at $\lambda = 18.9$nm.

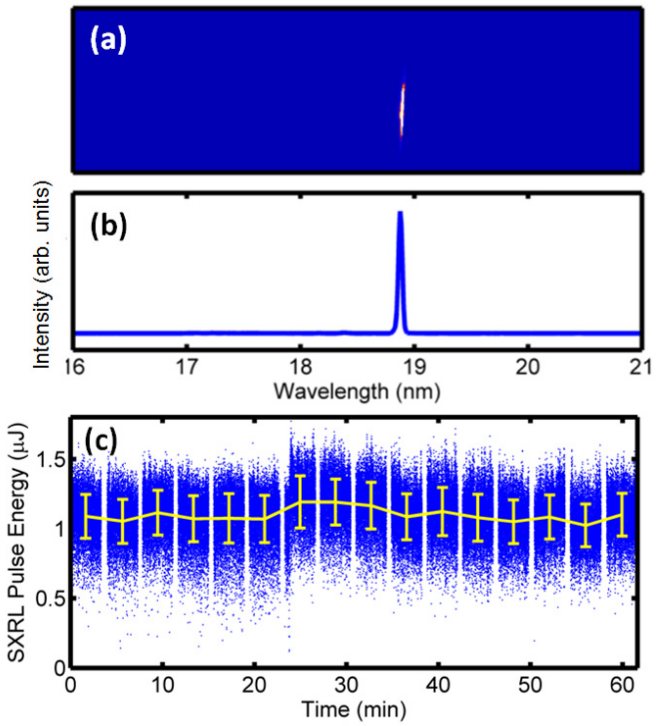

Fig. 2. (a) and (b) show a single shot on axis EUV spectrum of the Mo plasma with strong lasing observed on the $\lambda = 18.9$nm transition. (c) Measured SXRL pulse energy at 50 Hz repetition rate for just over 1 hour of operation. 180,000 consecutive shots were recorded. The line shows the running average of the pulse energy with the error bars representing the shot to shot standard deviation of each section of pulse sequence. The periodic gaps in the data correspond to transfers of the data from a digitizing oscilloscope to a computer during which the laser continued to operate.

Measurements of the SXRL laser energy as a function of plasma length have shown that this laser is operating in the gain-saturated regime [18], where efficient energy extraction is achieved. By replacing the spectrometer with a 45° multilayer Mo-Si mirror designed for the SXRL wavelength and recording an image of the far-field laser mode, the 90% energy divergence of the laser was determined to be 8 milliradians parallel to the target surface and 9 milliradians perpendicular to the target surface. The divergence can be decreased to sub-mrad

#198284 - $15.00 USD Received 25 Sep 2013; revised 4 Nov 2013; accepted 4 Nov 2013; published 11 Nov 2013

values by seeding the plasma amplifier with highly coherent low energy high order harmonic pulses [26] or with the output of a second line focus plasma amplifier [27].

In order to record a large number of laser shots at high repetition rate we replaced the CCD in the spectrometer with an EUV-sensitive silicon photodiode placed in the spectral location corresponding to the laser wavelength as shown in Fig. 1. The sensor has an active area of 1 mm x 10 mm, ensuring that practically only the SXRL laser emission contributes to the measured signal, as verified by slightly moving the detector off the laser line position. Absolute energy measurements were determined using the transmittance of the thin metal foil measured in situ, the reported grating diffraction efficiency and photodiode responsivity. The photodiode signal was recorded by a digitizing oscilloscope interfaced to a computer for extensive data storage. When only one oscilloscope is used there are periodic gaps in the recorded data. To acquire data at 100 Hz repetition rate, two oscilloscopes were used to record the waveform of every shot under continuous operation, with one scope acquiring the photodiode signal while the other transfers its recorded data to the computer.

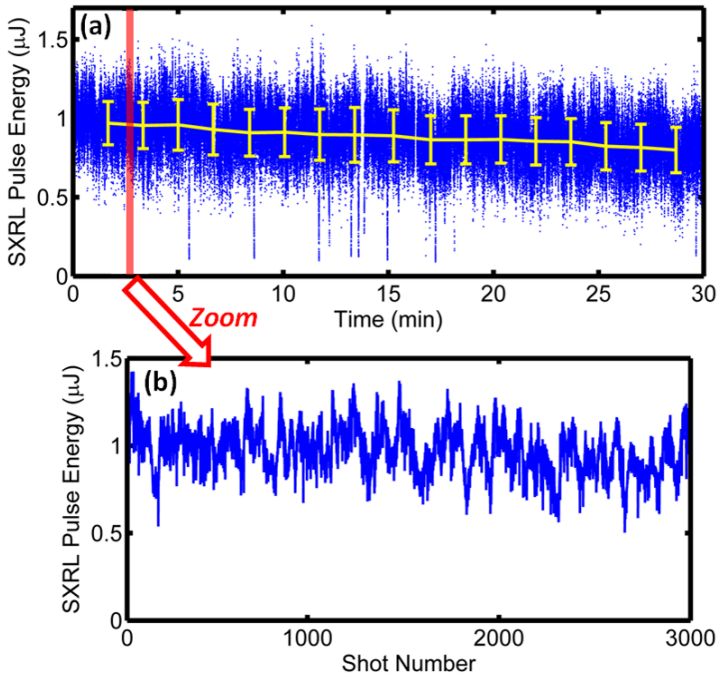

Fig. 3. (a) Recorded laser pulse energy variation for 30 minutes of continuous 100 Hz repetition rate operation of the λ = 18.9nm SXRL. The degradation of the pulse energy over the run is due to poor thermal stabilization of the lab causing a drift in the driver laser. (b) A close-up of the shaded 30 second subsection of the run in (a) showing the shot to shot stability of 3000 consecutive shots.

Figure 2(c) shows data corresponding to 1 hour of continuous operation of the λ = 18.9nm SXRL at 50 Hz repetition rate. The mean pulse energy is greater than 1 μJ, corresponding to > 50 μW average power. The laser output pulse energy is quite stable with very few low intensity shots. This continuous sequence of 1.8 x 10^5 shots was acquired with one rotation of the target of Fig. 1. Figure 3(a) shows the 30 minute operation of this laser at 100 Hz repetition rate with an average output power of about 0.1 mW. The slight degradation of the pulse energy over the run is due to poor thermal stabilization of the lab causing a drift in the driver laser. To acquire this data two digitizing oscilloscopes were used to record the photodiode signal eliminating most of the data transfer gaps. The shot to shot stability of this series is defined by a standard deviation of 16% over the entire 180,000 shots. This can be seen in the plot of Fig. 3(b), which shows a 3000 shot subset of the run. These

#198284 - $15.00 USD Received 25 Sep 2013; revised 4 Nov 2013; accepted 4 Nov 2013; published 11 Nov 2013

demonstrations, in which greater than 100 mJ of λ = 18.9 nm laser energy were delivered from a single target, show that this laser is an enabling tool for applications requiring a coherent high average power source.

4. Coherent soft x-ray laser-based nano-printing

As a demonstration of the use of this laser in applications requiring high photon flux we printed an array of nanometer-scale features through coherent Talbot lithography. The photo-lithographic approach used in this experiment is based on the self-imaging produced when a periodic transmission mask is illuminated with a coherent light beam. A semitransparent mask composed of an array of tiles each having an arbitrary design produces self images that replicate the mask on the surface of a photoresist [28]. This coherent imaging technique is an extension of the classical Talbot effect that can be explained by diffraction theory in the Fresnel approximation. This approach has also been used to lithographically print photonic

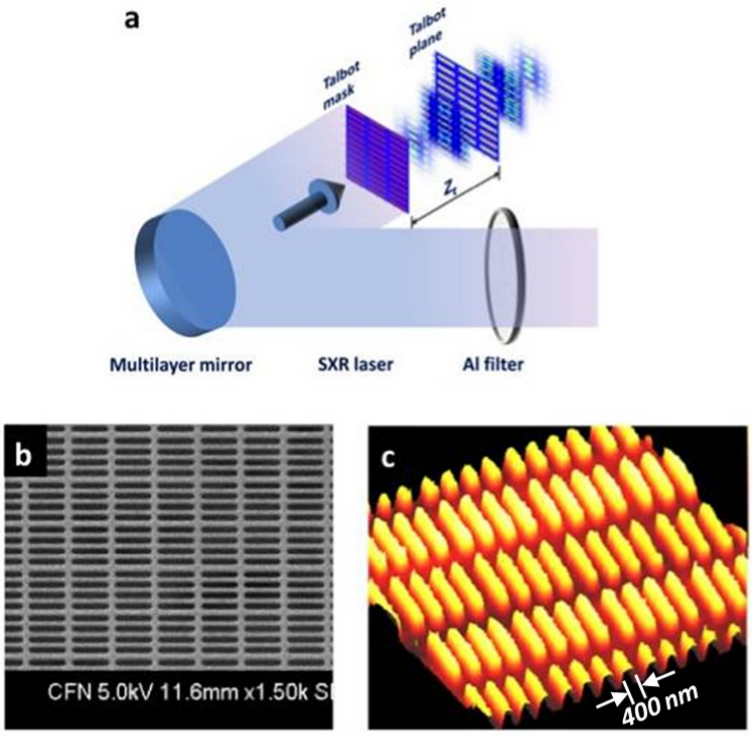

Fig. 4. (a) Talbot lithography experimental setup. The SXRL beam passes through an Al filter and impinges a 45° angle of incidence Mo-Si multilayer mirror. A two dimensional periodic mask generates a Talbot image at the sample plane that is registered in photoresist. (b) Scanning electron microscope (SEM) image of the Talbot mask defined on a SiN membrane. (c) Atomic force microscope image of the nanometer-scale features printed through Talbot lithography using the λ = 18.9 nm laser. The overall size of the array was ≈0.5 mm x 0.5 mm, and the width of the printed lines was ≈400 nm.

crystal structures in what was called coherent diffraction lithography [29]. When illuminated with coherent light, the tiled diffractive mask produces images which are 1 × replicas at certain locations (Talbot planes). Because the Talbot images are generated by the diffraction of the thousands of cells in the mask, a defect in any of the unitary cells is averaged over a very large numbers of tiles consequently rendering a virtually defect-free image.

Figure 4(a) shows the scheme of the experimental setup used to demonstrate Talbot printing. The soft x-ray laser beam was reflected by a 45° angle of incidence Mo-Si multilayer mirror that allowed for alignment of the system and provided extra wavelength filtering due to

#198284 - $15.00 USD Received 25 Sep 2013; revised 4 Nov 2013; accepted 4 Nov 2013; published 11 Nov 2013

the narrowband reflectivity of the multilayer coating centered at the laser wavelength. At the first Talbot plane a substrate coated with AZPN photoresist was placed to record the image. The mask was composed of 10,000 unit cells arranged in a square matrix with a period p = 5 μm. Each cell consisted of 4 slits 500 nm width and 1.2 μm period. A scanning electron microscope (SEM) scan of the mask is shown in Fig. 4(b). The overall size of the mask is 0.5 × 0.5 mm^2, with a calculated first Talbot distance Z_T = 2.65 mm. However, the print was made at half this distance where a phase-shifted Talbot image is produced, yielding a numerical aperture (NA) of 0.186. Figure 4(c) is an atomic force microscope image of the print in the photoresist. The features of the mask are adequately replicated in the photoresist surface. The FWHM width of the lines is ~400nm. The high flux of the soft x-ray laser allowed for efficient printing. The print was obtained with an exposure of 30 s operating the laser at 50 Hz repetition rate. The NA of this mask should allow for an image resolution of 50 nm, however, smaller feature sizes might be printed taking advantage of the non-linear response of the resist Ultimately, the short wavelength of this laser in combination with masks of larger NA could lead to defect-free printing of patterns with sub-20 nm feature sizes.

5. Conclusions

In summary, we have demonstrated the continuous operation of a compact λ = 18.9 nm SXRL at 100 Hz repetition rate for extended periods of time. Combining a soft x-ray plasma amplifier heated by a diode-pumped Yb:YAG laser driver with a high shot-capacity rotating target, we demonstrated the uninterrupted generation of a λ = 18.9 nm laser with ~0.1 mW average power for 30 minutes. This corresponds to over 1.8 x 10^5 consecutive shots. As a demonstration of the utility of this laser in applications requiring a high average photon flux we printed an array of nanometer-scale features through coherent lithography. This is the first demonstration of Talbot nano-printing using a compact sub-20nm wavelength coherent source. These results can be scaled to several hours of continuous operation and to shorter wavelengths. Compact high average power soft x-ray lasers can be expected to open the door to numerous photon flux intensive applications on a tabletop.

Acknowledgments

This work was supported by the National Science Foundation Engineering Research Center for Extreme Ultraviolet Science and Technology using equipment developed with NSF MRI grant 0521649, and by the AMOS program of the Office of Basic Energy Sciences, U.S. Department of Energy. We thank Eric Gullikson for the fabrication of the multilayer mirror. We also acknowledge the contributions to the early stages of the development of this laser by Bradley M. Luther, Federico J. Furch and Alden. H. Curtis. A previous collaboration with Abby Weith and James Dunn in the development of rotating targets is acknowledged. The multilayer coatings for the driver laser were developed by Dinesh Patel and Carmen S. Menoni with the support of the Office of Naval Research and the High Energy Laser Program of the DoD Joint Technology Office.